Food Analytical Methods (2019) 12:1666–1673
https://doi.org/10.1007/s12161-019-01509-4

Silver Nanoplates and Gold Nanospheres as Probesfor Revealing an "Interference" Phenomenon in a Simultaneous Quantitative Immunochromatographic Assay

Ganggang Zhang[1] · Youju Huang[2,3] · Juan Peng[1] · Jiaojiao Han[1] · Ping Guo[4] · Lei Zhang[2] · Jiawei Zhang[2] · Weihua Lai[1] · Tao Chen[2,3]

Received: 17 January 2019 / Accepted: 10 April 2019 / Published online: 30 April 2019

Abstract

Escherichia coli O157:H7 and *Salmonella choleraesuis* are two important foodborne pathogens that cause illnesses and even deaths. Rapid and convenient methods, such as immunochromatographic assays (ICAs), are useful for detecting these two pathogens. Herein, we developed a highly sensitive ICA for the simultaneous quantitative analysis of these two foodborne pathogens. Silver nanoplates (AgNPs) and gold nanospheres (AuNSs) were synthesized as two probes for simultaneous detection. In this method, *Escherichia coli* O157:H7 (*E. coli* O157:H7) and *Salmonella choleraesuis* (*S. choleraesuis*) were specifically detected at concentrations as low as 2.16×10^4 and 1.18×10^5 colony-forming units (CFU)/mL, respectively, in 30 min. Subsequently, a method for separately detecting these two targets with the same test strips was developed. The tests achieved specific detections of *E. coli* O157:H7 and *S. choleraesuis*, with detection limits of 1.07×10^4 and 9.85×10^4 CFU/mL, respectively. By comparing the intensity of the test lines (*T*) in the two methods, we found an interesting phenomenon in which the intensity of *T* in the simultaneous detection method was lower than that in the separate detection method. RGB analysis of the test lines demonstrated that the two probe–target compounds influenced each other. We believe that this phenomenon is an important factor to consider when building a simultaneous quantitative ICA.

Keywords *Escherichia coli* O157:H7 · *Salmonella choleraesuis* · Interference · Silver nanoplates · Gold nanospheres · Simultaneous quantitative immunochromatographic assay

Introduction

Diseases caused by pathogens greatly harm human health and social stability. According to the reports from the Centers for Disease Control and Prevention from 2015 to 2016 (NORS 2018), the number of illness cases caused by pathogens was 29,754, among which two pathogens, namely, *Escherichia coli* O157:H7 (*E. coli* O157:H7) (CDC 2017) and *Salmonella choleraesuis* (*S. choleraesuis*) (CDC 2018), are crucial. *E. coli* O157:H7 is a dangerous foodborne pathogen given its low infectious dose (minimum of 10 viable cells) (Guo et al. 2016). *S. choleraesuis* usually causes systemic infection in humans, as well as bacteremia and metastatic focal infections (Cohen et al. 1987).

The conventional culture method is the gold standard for detecting pathogens, but is labor intensive and time consuming, with some standardized procedures requiring up to 7 days (Boer and Rijkelt 1999). Polymerase chain reaction (Cao et al. 2017; Hsu et al. 2013; Shu et al. 2017; Xie et al. 2016) and enzyme-linked immunosorbent assay (ELISA) (Charlermroj

Electronic supplementary material The online version of this article (https://doi.org/10.1007/s12161-019-01509-4) contains supplementary material, which is available to authorized users.

✉ Youju Huang
yjhuang@nimte.ac.cn

✉ Weihua Lai
talktolaiwh@163.com

✉ Tao Chen
tao.chen@nimte.ac.cn

[1] State Key Laboratory of Food Science and Technology, Nanchang University, Nanchang 330047, China

[2] Key Laboratory of Marine Materials and Related Technologies, Zhejiang Key Laboratory of Marine Materials and Protective Technologies, Ningbo Institute of Material Technology and Engineering, Chinese Academy of Sciences, Ningbo 315201, China

[3] University of Chinese Academy of Sciences, 19A Yuquan Road, Beijing 100049, China

[4] Jiangxi Food Inspection and Testing Research Institute, Nanchang, Jiangxi Province, China

et al. 2014; Hsu et al. 2014; Wei et al. 2016; Xue et al. 2013) are the most commonly used methods. However, these two methods are limited by the disadvantages of complicated operation, the need for sample preparation, and long analysis time. Immunochromatographic assays (ICAs) (Morales-Narvaez et al. 2015; Park et al. 2016; Raeisossadati et al. 2016; Shan et al. 2015) are also broadly used to detect pathogens because of the advantages of speed, simplicity, and low cost.

Traditional ICA usually detects only one target and is thus inefficient in actual sample detection. A series of simultaneous quantitative ICAs have emerged and are being thoroughly developed in many fields. A 10-channel upconverting phosphor technology-based lateral flow (TC-UPT-LF) assay (Zhao et al. 2016) was developed for the rapid and simultaneous detection of ten epidemic foodborne pathogens. Ten different single-target UPT-LF strips were developed and integrated into one optimized TC-UPT-LF disk. Without enrichment, the TC-UPT-LF assay has a detection sensitivity of 10^4 or 10^5 colony-forming units (CFU)/mL for each pathogen; this sensitivity becomes 10 CFU/0.6 mg after sample enrichment. An ICA for multiplex pathogen detection was developed (Park et al. 2010). Optical (colorimetric) signal can be successfully generated using the proposed immunostrip system to selectively detect four different pathogens. The detection ranges of the immunostrips for *Salmonella typhimurium*, *Staphylococcus aureus*, *Legionella pneumophila*, and *E. coli* O157:H7 were determined to be 9.2×10^3 CFU/mL to 9.2×10^5 CFU/mL, 8.7×10^4 CFU/mL to 8.7×10^6 CFU/mL, 1.3×10^3 CFU/mL to 1.3×10^5 CFU/mL, and 1.2×10^5 CFU/mL to 1.2×10^7 CFU/mL, respectively. The simultaneous quantitative ICA is the current trend in food safety analysis.

In this work, we developed an ICA that simultaneously detects *E. coli* O157:H7 and *S. choleraesuis* by using two probes of different colors (silver nanoplates (AgNPs) and gold nanospheres (AuNSs)). The two probe–target complexes interfered with each other on the test line and resulted in a decreased signal. This effect can influence the accuracy of the ICA for simultaneously quantifying pathogens. A study based on two probe–target complexes that affect the test lines in a simultaneous quantitative ICA is first reported herein.

Materials and Methods

Materials and Equipment

E. coli O157:H7 (ATCC 43888) was cultured in Luria–Bertani medium (LB; Oxoid, Basingstoke, UK) at 37 °C for 20 h before use. *S. choleraesuis* (ATCC 10708) was inoculated in a solid LB medium plate and then cultured at 37 °C overnight. *Listeria monocytogenes* (*L. monocytogenes*), *Shigella*, and *Staphylococcus aureus* (*S. aureus*) were obtained from the Jiangxi CDC. Hydrogen tetrachloroaurate trihydrate ($HAuCl_4 \cdot 3H_2O$), sodium citrate (SC), sodium borohydride ($NaBH_4$), 1-ethyl-3-(3-dimethylaminopropyl) carbodiimide (EDC), and N-hydroxysulfosuccinimide sodium salt (NHSS) were obtained from Aldrich (Milwaukee, WI). 11-Mercaptoundecanoic acid (MUA), H_2O_2 (30 wt%), casein, polyethylene glycol 20000 (PEG_{20000}), phosphate-buffered saline (PBS, 0.01 M, pH = 7.4), bovine serum albumin (BSA), and boric acid buffer (BB, pH = 8) were purchased from Sigma. Milk was purchased from the Rainbow Supermarket in Nanchang, China. All the antibodies were obtained from our previous studies. The sample pad, nitrocellulose membrane, and absorbent pad were purchased from Millipore, Inc. (Bedford, MA). All solvents and other chemicals were of analytical reagent grade.

The BioDot XYZ platform, which combines motion control with the BioJet Quanti3050k dispenser and AirJet Quanti3050k dispenser, was acquired from BioDot (Irvine, CA). Gray-scale intensity strip readers were purchased from Shanghai Huguo Science Instrument Co., Ltd. (China).

Synthesis of AgNPs and MUA-Modified AgNPs (Ag-MUA)

Briefly, $AgNO_3$ (120 μL, 0.1 M), SC (1800 μL, 0.1 M), and H_2O_2 (30 wt%, 336 μL) were mixed with water (final volume: 120 mL) at room temperature and vigorously stirred for 10 min. Then, $NaBH_4$ (100 mM, 1200 μL, freshly prepared with cold water) was rapidly injected into this mixture, and the solution changed gradually from colorless to yellow, red, and blue, which indicates the formation of AgNPs. The resultant triangular nanoplate solution was stored at 4 °C overnight before use.

To obtain the Ag-MUA complex, we added 12 mL of MUA (0.02 M, pH = 10, freshly prepared) to the AgNP solution (120 mL) dropwise and stirred in the dark for 48 h. Then, the mixture was centrifuged at 11,000 r/min and 4 °C for 25 min. The supernatant was discarded, and the resulting precipitate was redissolved in 36 mL of BB.

Synthesis of AuNSs

$HAuCl_4$ stock solution (1 mL, 1% wt/vol) was added to 99 mL of ultrapure water and heated to its boiling point. Then, 1.45 mL of SC solution (freshly prepared, 1%) was added to the gold solution with constant stirring. When the color of the mixture turned red, the mixture was boiled continuously and stirred for another 30 min. The colloidal gold solution was then cooled to room temperature and stored at 4 °C.

Preparation of the Ag-MUA-Monoclonal Antibody (Ag-MUA-mAb) and AuNS-Monoclonal Antibody (Au-mAb)

To obtain the Ag-MUA-mAb, we added 0.2 mL of anti-*E. coli* O157:H7 monoclonal antibody solution dropwise to 2 mL of Ag-MUA to a final concentration of 10 μg/mL with gentle stirring for 60 min. Then, 0.2 mL of casein (2% wt/vol) was added for blocking in the dark for 4 h. The resulting solution was centrifuged at 9000 r/min at 4 °C for 30 min. The supernatant was then discarded to remove the unreacted free antibody, and the resultant precipitate was redissolved in 200 μL of dilution buffer.

A total of 2 mL of colloidal gold solution was adjusted to pH 8.0 by using 0.2 M K_2CO_3. Afterward, 0.2 mL of an anti-*S. choleraesuis* monoclonal antibody solution was added dropwise to the colloidal gold solution to a final concentration of 5 μg/mL with gentle stirring for 60 min. Subsequently, 0.2 mL of PEG_{20000} solution (1%) was added to the solution and stirred for 30 min. Afterward, 0.2 mL of BSA (10% wt/vol) was added for further blocking for 30 min. The resultant solution was centrifuged at 8000 r/min and 4 °C for 30 min. The supernatant was discarded to remove the unreacted free antibody, and the resulting precipitate was redissolved in 200 μL of dilution buffer.

Preparation of the Immunochromatographic Test Strips

The anti-*E. coli* O157:H7 monoclonal antibody, anti-*S. choleraesuis* polyclonal antibody, and goat anti-mouse antibody were diluted with PBS (0.01 M) to final concentrations of 0.8, 1.2, and 0.6 mg/mL, respectively. The three mixtures were then applied to the two test lines (T_1 and T_2) and control lines (C) on the nitrocellulose membrane and dried at 30 °C overnight. The nitrocellulose membrane, absorption pad, and pretreated sample pad were assembled as the test strip (Fig. 1).

Separate Detection of *E. coli* O157:H7 and *S. choleraesuis*

PBS was spiked with *E. coli* O157:H7 at the concentrations of 0, 1×10^4, 2×10^4, 1×10^5, 2×10^5, 1×10^6, and 2×10^6 CFU/mL. A total of 100 μL of the solution was added to the ELISA plate well, in which 10 μL of Ag-MUA-mAb was added. After 3 min of incubation, the mixture was added to the sample pad of the test strip. After 25 min, the test line (T_1) was read to detect the signal. A calibration curve was constructed by plotting T_1 as the ordinate (Y) and the *E. coli* O157:H7 concentration (c) as the abscissa (X). Information on the linear regression equation was established for quantitative analysis. The T_1 line (at 2×10^5 CFU/mL) was cut, and the RGB histogram was obtained by MATLAB and ImageJ.

Similarly, PBS was spiked with *S. choleraesuis* at concentrations of 0, 1×10^5, 2×10^5, 1×10^6, 2×10^6, 1×10^7, and 2×10^7 CFU/mL. A total of 100 μL of the solution was added to the ELISA plate well, in which 5 μL of Au-mAb was added. After 3 min of incubation, the mixture was added to the sample pad of the test strip. After 25 min, the test line (T_2) was read to detect the signal. The calibration curve was constructed by plotting T_2 as the ordinate (Y) and the concentration of *S. choleraesuis* (c) as the abscissa (X). Information of the linear regression equation was established for quantitative analysis. The T_2 line (at 2×10^6 CFU/mL) was cut, and the RGB histogram was obtained by MATLAB and ImageJ

Simultaneous Detection of *E. coli* O157:H7 and *S. choleraesuis*

PBS was spiked with *E. coli* O157:H7 and *S. choleraesuis* at concentrations of (0, 0), (1×10^4, 1×10^5), (2×10^4, 2×10^5), (1×10^5, 1×10^6), (2×10^5, 2×10^6), (1×10^6, 1×10^7), and (2×10^6, 2×10^7) CFU/mL. Then, 100 μL of

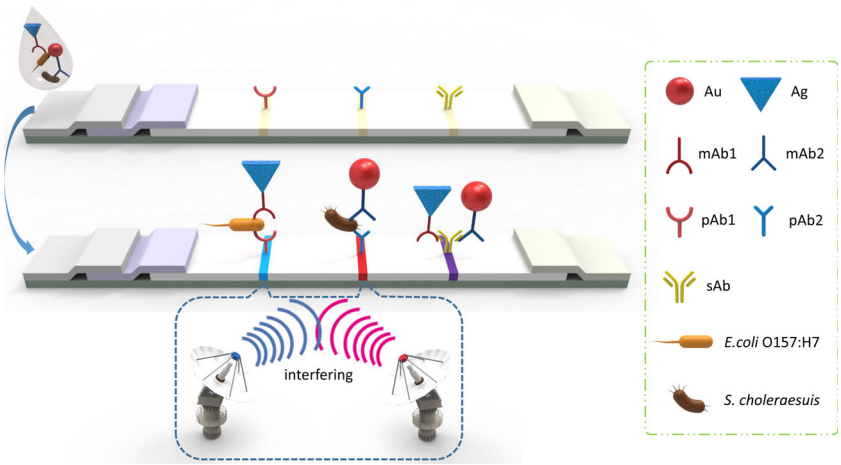

Fig. 1 Schematic of the immunochromatographic strip simultaneously quantifying *E. coli* O157:H7 and *S. choleraesuis* based on AgNPs and AuNSs

the solution was added to the ELISA plate well, in which 10 μL of Ag-MUA-mAb and 5 μL of Au-mAb were added. After 3 min of incubation, the mixture was added to the sample pad of the test strip. After 25 min, the test lines (T_1 and T_2) were read to detect the signal. The calibration curve was constructed by plotting the T as the ordinate (Y) and the concentration (c) as the abscissa (X). Information on the linear regression equation was established for quantitative analysis. The T_1 and T_2 lines (at 2×10^5 CFU/mL of *E. coli* O157:H7 and 2×10^6 CFU/mL of *S. choleraesuis*) were cut, and the RGB histogram of T_1 and T_2 was obtained by MATLAB and ImageJ.

Specificity Experiments

The specificity experiments for the ICA were conducted as follows. PBS was spiked with *E. coli* O157:H7, *S. choleraesuis*, *L. monocytogenes*, *Shigella*, and *S. aureus* at 1×10^6 CFU/mL. The spiked PBS was detected through simultaneous ICA.

Analysis of Milk Sample

E. coli O157:H7- and *S. choleraesuis*-negative milk samples were spiked with *E. coli* O157:H7 and *S. choleraesuis* at (1×10^4, 1×10^5), (1×10^5, 1×10^6), and (1×10^6, 1×10^7) CFU/mL. The spiked milk samples were detected through simultaneous ICA.

Results and Discussion

Principle of the Method

In this work, we provided an ICA that simultaneously quantifies two targets by using two different probes (Fig. 1). A Ag-MUA-labeled anti-*E. coli* O157:H7 monoclonal antibody and a AuNS-labeled anti-*S. choleraesuis* monoclonal antibody were employed as the two probes (Ag-MUA-mAb and Au-mAb). Then, the anti-*E. coli* O157:H7 monoclonal antibody, anti-*S. choleraesuis* polyclonal antibody, and goat anti-mouse antibody were immobilized on a nitrocellulose membrane as T_1, T_2, and C, respectively. When the two targets were present in a sample, the complexes of Ag-MUA-mAb–*E. coli* O157:H7 and Au-mAb–*S. choleraesuis* were captured by T_1 and T_2, respectively. The two complexes could interfere with each other as two signals. This interference will result in a decreased signal, as detected by gray-level comparative analysis and RGB analysis.

Characterization of AgNPs and AuNSs

AgNPs and AuNSs were used for their differences in shape and color. The transmission electron microscopy (TEM) images reveal an average diameter of 40 nm for the AgNPs and 20 nm for the AuNSs (Fig. S1).

To maintain the shape of AgNPs and distinguish them from AuNSs, we adopted MUA. The (110) facets possess a lower coordination number than the (111) facets. This discrepancy

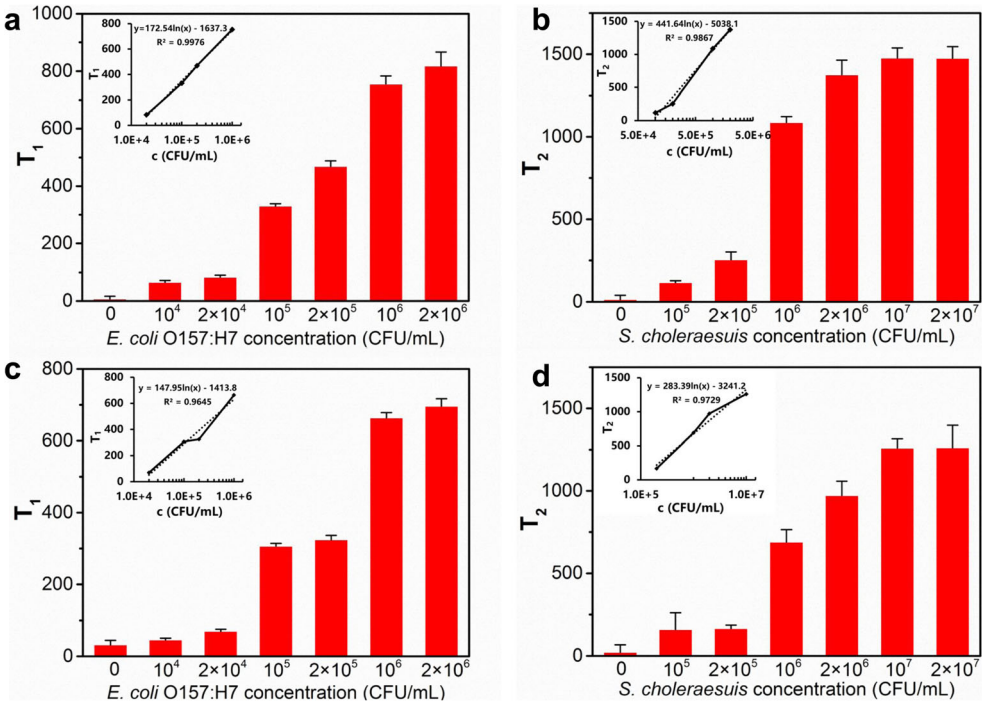

Fig. 2 Quantitative calibration curve. Separate detection of **a** *E. coli* O157:H7 based on AgNPs, and separate detection of **b** *S. choleraesuis* based on AuNSs, simultaneous detection of **c** *E. coli* O157:H7, and **d** *S. choleraesuis* based on AgNPs and AuNSs, respectively

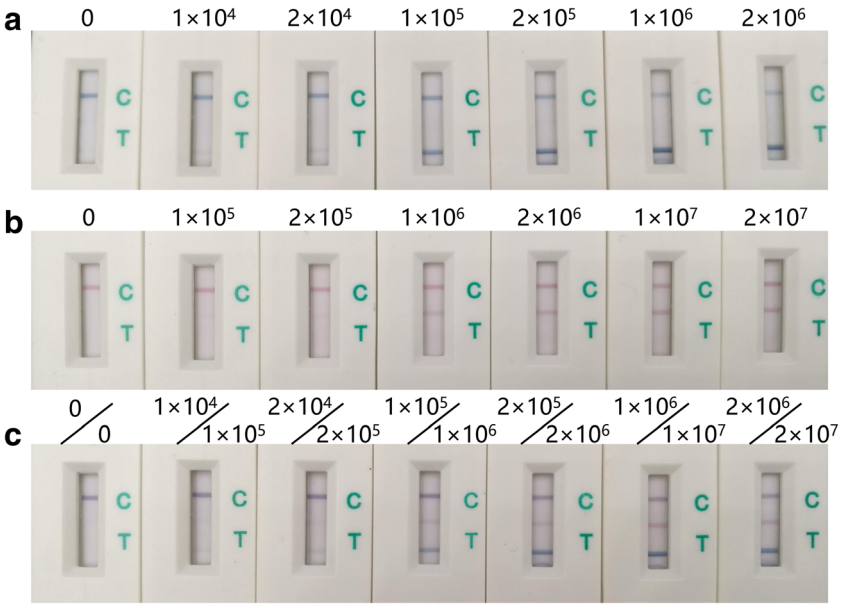

Fig. 3 Test results. **a** Separate detection of *E. coli* O157:H7 (CFU/mL) based on AgNPs, **b** separate detection of *S. choleraesuis* (CFU/mL) based on AuNSs, and **c** simultaneous detection of *E. coli* O157:H7 (CFU/mL) and *S. choleraesuis* (CFU/mL) based on AgNPs and AuNSs

resulted in an increased surface energy in these areas of the AgNPs. Therefore, the edges of the AgNPs were more prone to etching than other areas (Li et al. 2014). As shown in Fig. S2 (a, b), the edges of the AgNPs were etched. The sulfhydryl group (−SH) in MUA can bind Au by forming Au − S, and the carboxyl group (−COOH), which is located on the other end of MUA can bind an antibody by forming an amide bond (CONH). The λ_p (peak wavelength) of the AgNPs was 720 nm, whereas that of the Ag-MUA was 764 nm (Fig. S3). This result suggests that the AgNPs were successfully modified by MUA. Moreover, MUA successfully protected the AgNPs (Fig. S2 (c, d)).

Characterization of the Ag-MUA-mAb and Au-mAb Immunonanocomplex

Commonly, the absorbance peak of the immunonanocomplex red shifts relative to that of nanoparticles because the size of the immunonanocomplex is larger than that of the nanoparticles. The λ_p of the Ag-MUA was 764 nm, and that of the Ag-MUA-mAb was 779 nm, with a 15 nm red shift (Fig. S4a). In addition, the λ_p of the AuNSs was 523 nm, and that of the Au-mAb was 530 nm, with a 7 nm red shift (Fig. S4b). These results indicate that the two antibodies were bound to the surface of the two nanoparticles.

Quantitative Calibration Curve

Serially spiked samples were detected using the ICA test strip to establish the calibration curve (Fig. 2). The calibration curve was constructed by plotting the intensity of *T* as the ordinate (*Y*) and the concentrations of pathogen (*c*) as the abscissa (*X*). The curves of separate detection and simultaneous detection exhibited good linearity, and the coefficient of variation for each concentration was less than 12.2% (Table S2). The limit of detection (LOD) was calculated by finding the concentration at which the signal–noise ratio was three ($S/N = 3$). The nonlinear fitting equations and LOD values are listed in Table S1.

In a comparison of the separate detection (Fig. 2a) and simultaneous detection (Fig. 2c) of *E. coli* O157:H7, the LOD of the latter (2.16×10^4 CFU/mL) was approximately

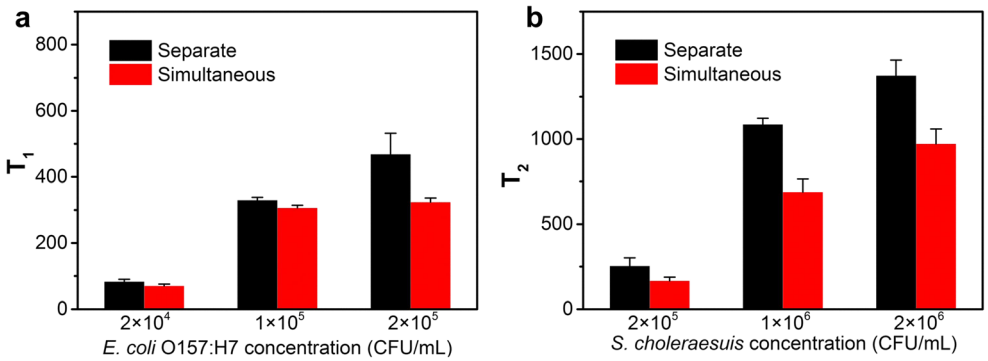

Fig. 4 Gray-level comparative analysis between separate and simultaneous detections. **a** Detection of *E. coli* O157:H7 based on AgNPs. **b** Detection of *S. choleraesuis* based on AuNSs

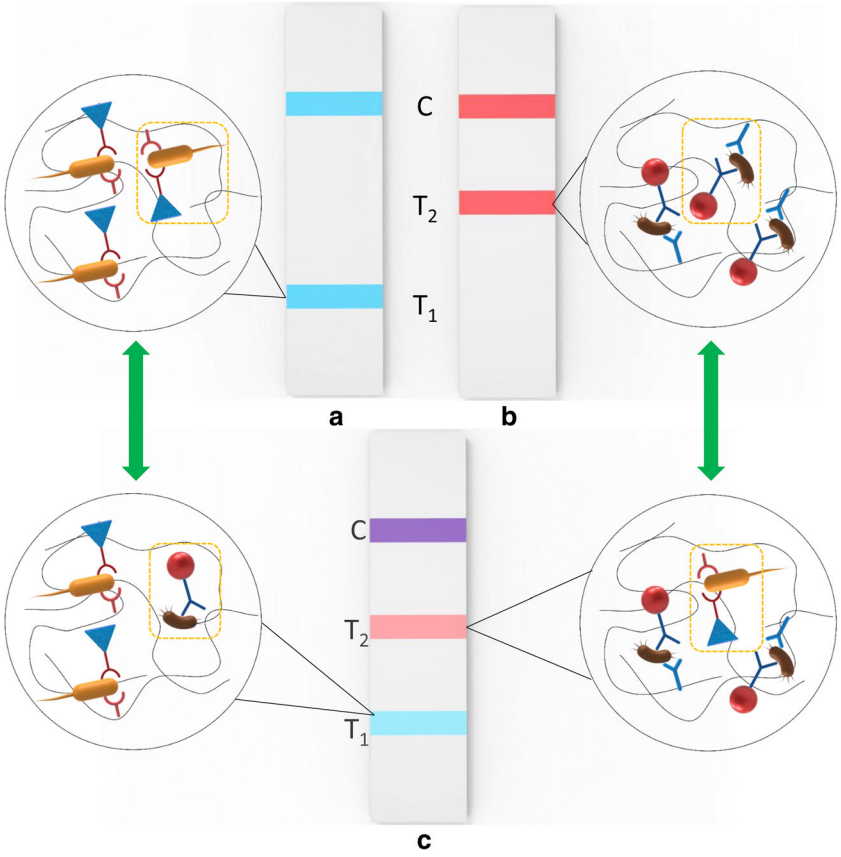

Fig. 5 Interference between two test lines in the immunochromatographic strip. **a** Separate detection of *E. coli* O157:H7 (CFU/mL) based on AgNPs, **b** separate detection of *S. choleraesuis* (CFU/mL) based on AuNSs, and **c** simultaneous detection of *E. coli* O157:H7 (CFU/mL) and *S. choleraesuis* (CFU/mL) based on AgNPs and AuNSs

twofold greater than that of the former (1.07×10^4 CFU/mL). Moreover, the LOD of simultaneous detection (1.18×10^5 CFU/mL, Fig. 2d) of *S. choleraesuis* was also higher than that of separate detection (9.85×10^4 CFU/mL, Fig. 2b). This result means that simultaneous detection leads to a lower sensitivity than separate detection. The result picture of the test strips is shown in Fig. 3. Compared with other reported work (Table S3), this method is convenient and rapid.

Specificity Experiments

The specificity of the simultaneous ICA was determined by evaluating cross-reactivity with frequently occurring foodborne pathogens, including *L. monocytogenes*, *Shigella*, and *S. aureus*. As shown in Fig. S7, the simultaneous ICA exhibited negligible cross-reactivities with other pathogens (< 2.8%).

Milk Sample Analysis

The results for the analytical recovery of two pathogens spiked into a milk sample are given in Table S4. The average recovery values ($n = 4$) ranged from 89.47 to 121.09%, with CV values between 9.1 and 15.4%.

Gray-Level Comparative Analysis

As the calibration curve was constructed by plotting the intensity of T as the ordinate (Y), the influence of the intensity of T was the key factor in this method's sensitivity. As shown in Fig. 4 and Fig. S5, the gray level of T in separate detection was higher than that in simultaneous detection, regardless of whether the AgNPs (T_1) or AuNSs (T_2) were utilized. Furthermore, the D value (difference value) increased with increasing concentration. When the concentrations of *E. coli* O157:H7 were 2×10^4, 1×10^5, and 2×10^5 CFU/mL, the D values were 13, 15, and 144, respectively. When the concentrations of *S. choleraesuis* were 2×10^5, 1×10^6, and 2×10^6 CFU/mL, the D values were 87, 397, and 402, respectively. These results imply that a higher pathogen concentration leads to a greater difference between separate detection and simultaneous detection.

ICA is commonly based on specific antigen–antibody binding and capillary effects. A higher pathogen concentration results in the formation of more probe–target complexes (Ag-MUA-mAb–*E. coli* O157:H7 and Au-mAb–*S. choleraesuis*). By contrast, while the complexes were moving on the nitrocellulose membrane (Fig. 5), the existence of Au-mAb–*S. choleraesuis* influenced the bonding T_1 capability of Ag-MUA-mAb–*E. coli* O157:H7 (Fig. 5a and Fig. 5c) and vice versa (Figs. 5b, c). This phenomenon occurs if nonspecific

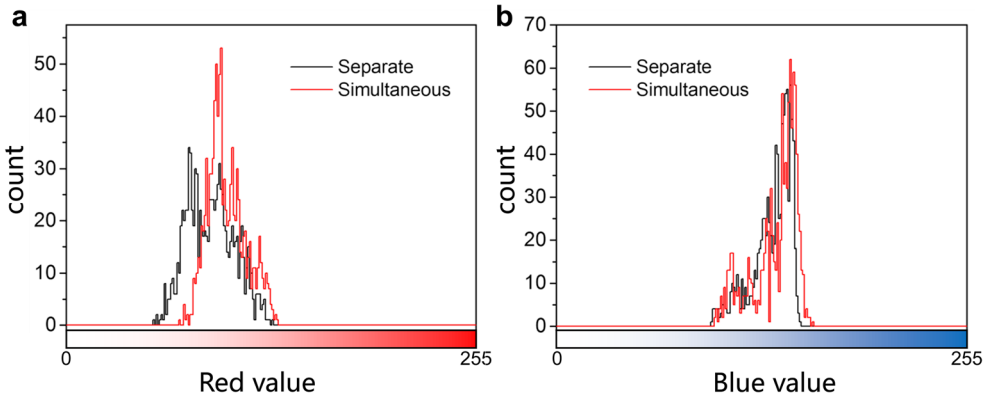

Fig. 6 Histogram of the red and blue channels. **a** Comparison of the separate and simultaneous detection for T_1. **b** Comparison of the separate and simultaneous detection for T_2. The *E. coli* O157:H7 concentration was 2×10^5 CFU/mL, and the *S. choleraesuis* concentration was 2×10^6 CFU/mL

adsorption is generated without cross-reaction between the two targets, as demonstrated by separate detection (Fig. 3a and b).

RGB Analysis

To demonstrate the generation of nonspecific adsorption, we analyzed the RGB of the two test lines. Given that the two nanoparticles used as labeled carriers were different colors, the interference between the two test lines was easily and accurately calculated (Fig. S6). At 2×10^5 CFU/mL *E. coli* O157:H7 and 2×10^6 CFU/mL *S. choleraesuis* (Fig. 6a), the red value of simultaneous detection in T_1 was higher than that of separate detection. This result means that the compound of Au-mAb–*S. choleraesuis* existed in T_1 during the simultaneous detection of the two pathogens. Similarly, the compound of Ag-MUA–mAb-*E. coli* O157:H7 existed in T_2 during the simultaneous detection of the two pathogens. The blue value of simultaneous detection in T_2 was higher than that of separate detection (Fig. 6b).

Conclusion

Given their advantages of speed, simplicity, and low cost, simultaneous quantitative methods for foodborne pathogens are urgently needed. Simultaneous quantitative ICA is an urgently needed method. However, low accuracy and the inability to quantify results limit the wide usage of this method. Moreover, the interaction between the test lines is frequently neglected.

Herein, we developed a simultaneous quantitative ICA based on AgNPs and AuNSs to detect *E. coli* O157:H7 and *S. choleraesuis*. Two colors of probes (blue and red) were successfully synthesized and not only allowed dual-target detection but also confirmed the accurate analysis of the two test lines. The separate and simultaneous detection methods were compared in terms of gray-level comparison analysis of *T*. The findings indicate that high pathogen concentrations result in an "interference" phenomenon. Moreover, the influence between the two test lines can be quantified by utilizing these two different probes. Through this work, we could build a simultaneous quantitative ICA with greater accuracy. On the basis of the predictions, smaller probes and NC membranes with larger pore sizes may be good choice for reducing the "interference" effect.

Funding This work was supported by the free explore issue of State Key Laboratory of Food Science and Technology of Nanchang University (SKLF-ZZB-201719), the Open Project Program of State Key Laboratory of Food Science and Technology, Nanchang University (SKLF-KF-201616), earmarked fund for Jiangxi Agriculture Research System (JXARS-03), and Jiangxi Special Fund for Agro-scientific Research in the Collaborative Innovation (JXXTCX201703-1).

Compliance with Ethical Standards

Conflict of Interest Ganggang Zhang declares that he has no conflict of interest. Youju Huang declares that he has no conflict of interest. Juan Peng declares that she has no conflict of interest. Jiaojiao Han declares that she has no conflict of interest. Ping Guo declares that he has no conflict of interest. Lei Zhang declares that he has no conflict of interest. Jiawei Zhang declares that she has no conflict of interest. Weihua Lai declares that he has no conflict of interest. Tao Chen declares that he has no conflict of interest.

Ethical Approval This article does not contain any studies with human participants or animals performed by any of the authors.

Informed Consent Not applicable.

References

Boer ED, Rijkelt RB (1999) Methodology for detection and typing of foodborne microorganisms. Int J Food Microbiol 50:119–130

Cao L, Cui X, Hu J, Li Z, Choi JR, Yang Q, Lin M, Ying Hui L, Xu F (2017) Advances in digital polymerase chain reaction (dPCR) and its emerging biomedical applications. Biosens Bioelectron 90:459–474. https://doi.org/10.1016/j.bios.2016.09.082

CDC (2017) Multistate outbreak of *Shiga* toxin-producing *Escherichia coli* O157:H7 infections linked to I.M. Healthy brand SoyNut butter (final update). https://www.cdc.gov/ecoli/2017/o157h7-03-17/index.html. Accessed 4 May 2017

CDC (2018) Reports of active Salmonella outbreak investigations. https://www.cdc.gov/salmonella/outbreaks-active.html. Accessed 7 Dec 2018

Charlermroj R, Himananto O, Seepiban C, Kumpoosiri M, Warin N, Gajanandana O, Elliott CT, Karoonuthaisiri N (2014) Antibody array in a multiwell plate format for the sensitive and multiplexed detection of important plant pathogens. Anal Chem 86:7049–7056. https://doi.org/10.1021/ac501424k

Cohen JI, Bartlett JA, Ralph Corey G (1987) Extra-intestinal manifestations of *salmonella* infections. Medicine 66:349–388

Guo Q, Han JJ, Shan S, Liu DF, Wu SS, Xiong YH, Lai WH (2016) DNA-based hybridization chain reaction and biotin-streptavidin signal amplification for sensitive detection of *Escherichia coli* O157:H7 through ELISA. Biosens Bioelectron 86:990–995. https://doi.org/10.1016/j.bios.2016.07.049

Hsu HL, Huang HH, Liang CC, Lin HC, Liu WT, Lin FP, Kau JH, Sun KH (2013) Suspension bead array of the single-stranded multiplex polymerase chain reaction amplicons for enhanced identification and quantification of multiple pathogens. Anal Chem 85:5562–5568. https://doi.org/10.1021/ac400778b

Hsu CK, Huang HY, Chen WR, Nishie W, Ujiie H, Natsuga K, Fan ST, Wang HK, Lee JYY, Tsai WL, Shimizu H, Cheng CM (2014) Paper-based ELISA for the detection of autoimmune antibodies in body fluid-the case of bullous pemphigoid. Anal Chem 86:4605–4610. https://doi.org/10.1021/ac500835k

Li Y, Li Z, Gao Y, Gong A, Zhang Y, Hosmane NS, Shen Z, Wu A (2014) "red-to-blue" colorimetric detection of cysteine via anti-etching of silver nanoprisms. Nanoscale 6:10631–10637. https://doi.org/10.1039/c4nr03309d

Morales-Narvaez E, Naghdi T, Zor E, Merkoci A (2015) Photoluminescent lateral-flow immunoassay revealed by graphene oxide: highly sensitive paper-based pathogen detection. Anal Chem 87:8573–8577. https://doi.org/10.1021/acs.analchem.5b02383

NORS (2018) National Outbreak Reporting System Dashboard https://wwwn.cdc.gov/norsdashboard/. Accessed 7 Dec 2018

Park J, Park S, Kim Y-K (2010) Multiplex detection of pathogens using an immunochromatographic assay strip. BioChip J 4:305–312. https://doi.org/10.1007/s13206-010-4407-2

Park J, Shin JH, Park JK (2016) Pressed paper-based dipstick for detection of foodborne pathogens with multistep reactions. Anal Chem 88:3781–3788. https://doi.org/10.1021/acs.analchem.5b04743

Raeisossadati MJ, Danesh NM, Borna F, Gholamzad M, Ramezani M, Abnous K, Taghdisi SM (2016) Lateral flow based immunobiosensors for detection of food contaminants. Biosens Bioelectron 86:235–246. https://doi.org/10.1016/j.bios.2016.06.061

Shan S, Lai W, Xiong Y, Wei H, Xu H (2015) Novel strategies to enhance lateral flow immunoassay sensitivity for detecting foodborne pathogens. J Agric Food Chem 63:745–753. https://doi.org/10.1021/jf5046415

Shu B, Zhang C, Xing D (2017) A sample-to-answer, real-time convective polymerase chain reaction system for point-of-care diagnostics. Biosens Bioelectron 97:360–368. https://doi.org/10.1016/j.bios.2017.06.014

Wei T, Du D, Zhu MJ, Lin Y, Dai Z (2016) An improved ultrasensitive enzyme-linked immunosorbent assay using hydrangea-like antibody-enzyme-inorganic three-in-one nanocomposites. ACS Appl Mater Interfaces 8:6329–6335. https://doi.org/10.1021/acsami.5b11834

Xie X, Wang S, Jiang SC, Bahnemann J, Hoffmann MR (2016) Sunlight-activated propidium monoazide pretreatment for differentiation of viable and dead bacteria by quantitative real-time polymerase chain reaction. Environ Sci Technol Lett 3:57–61. https://doi.org/10.1021/acs.estlett.5b00348

Xue S, Li HP, Zhang JB, Liu JL, Hu ZQ, Gong AD, Huang T, Liao YC (2013) Chicken single-chain antibody fused to alkaline phosphatase detects Aspergillus pathogens and their presence in natural samples by direct sandwich enzyme-linked immunosorbent assay. Anal Chem 85:10992–10999. https://doi.org/10.1021/ac402608e

Zhao Y, Wang H, Zhang P, Sun C, Wang X, Wang X, Yang R, Wang C, Zhou L (2016) Rapid multiplex detection of 10 foodborne pathogens with an up-converting phosphor technology-based 10-channel lateral flow assay. Sci Rep 6:21342. https://doi.org/10.1038/srep21342